Talanta 90 (2012) 30–37

Contents lists available at SciVerse ScienceDirect

Talanta

journal homepage: www.elsevier.com/locate/talanta

Determination of the absolute fluorescence quantum yield of rhodamine 6G with optical and photoacoustic methods – Providing the basis for fluorescence quantum yield standards

Christian Würth[a], Martín G. González[b], Reinhard Niessner[b], Ulrich Panne[a,c], Christoph Haisch[b,*], Ute Resch Genger[a,**]

[a] BAM Federal Institute for Materials Research and Testing, Richard-Willstaetter-Str. 11, 12489 Berlin, Germany
[b] Institute of Hydrochemistry, Technische Universität München, Marchioninistr. 17, 81377 Munich, Germany
[c] Humboldt-Unversität zu Berlin, Department of Chemistry, Brook-Taylor-Str. 2, 124789 Berlin, Germany

ARTICLE INFO

Article history:
Received 18 September 2011
Received in revised form
14 December 2011
Accepted 18 December 2011
Available online 23 December 2011

Keywords:
Fluorescence
Photoluminescence
Quantum yield
Photoacoustic spectroscopy
Absolute quantum yield
Integrating sphere
Rhodamine 6G
Aggregation
Reabsorption

ABSTRACT

To establish the methodical basis for the development and certification of fluorescence quantum yield standards, we determined the fluorescence quantum yield Φ_f of rhodamine 6G (R6G) with two absolute methods with complementary measurement principles, here optical spectroscopy using an integrating sphere setup and pulsed laser photoacoustic spectroscopy (PAS). For the assessment of aggregation- and reabsorption-induced distortions of measured fluorescence quantum yields and procedures for the reliable consideration of such effects, this systematic comparison was performed in ethanol and in water employing different concentrations of R6G. In addition, the relative and absolute fluorescence quantum yields of these solutions were obtained with a calibrated spectrofluorometer and a commercialized integrating sphere setup. Based upon this systematic comparison, experimental advantages and systematic sources of variation were identified for both methods.

© 2012 Published by Elsevier B.V.

1. Introduction

For any photoluminescent species, the quantum yield of its luminescence (Φ_f) presents one of its most fundamental properties [1,2]. This quantity provides a direct measure for the efficiency of the conversion of absorbed photons into emitted photons. Moreover, the brightness, i.e., the product of the dye's molar decadic absorption coefficient ε at the excitation wavelength and Φ_f, is a frequently used spectroscopic measure for the comparison of functional fluorophores [3]. Hence, the measurement of Φ_f is a key step in the characterization of any photoluminescent species. The reliable determination of Φ_f is, however, still challenging even for transparent chromophore solutions, as Φ_f is affected by many different parameters such as temperature, dye environment (solvent polarity, proticity, and viscosity of the matrix), and dye concentration in the case of aggregating chromophores as well as by the presence of potential quenchers (e.g., oxygen).

According to the definition of Φ_f, principally only two quantities need to be measured for its calculation, see Eq. (1), the number of photons absorbed (N_{abs}) and the number of photons emitted (N_{em}). For transparent dye solutions, the most elementary method for the determination of Φ_f involves the comparison of the integrated, spectrally corrected fluorescence intensity of a dilute fluorophore solution with that of a solution of a quantum yield standard of known Φ_f under identical measurement conditions using conventional absorption and fluorescence spectrometers [4–9]. Pitfalls of this frequently used relative optical method are the mandatory determination of spectral correction curves to account for wavelength-dependent instrument-specific signal contributions, polarization effects, and the Φ_f value used for the standard [4,5,10–15]. With proper consideration of these sources of systematic error, relative uncertainties of 6% can be accomplished if the fluorescence quantum yield of the standard is reliably known [4,10]. Despite the intense research dedicated to quantum yield standards, according to a very recent review, only

* Corresponding author. Tel.: +49 89 2180 78242; fax: +49 89 2180 99 78242.
** Corresponding author.
E-mail addresses: ute.resch@bam.de, christoph.haisch@ch.tum.de (C. Haisch).

0039-9140/$ – see front matter © 2012 Published by Elsevier B.V.
doi:10.1016/j.talanta.2011.12.051

three fluorophores recommended in the literature can be currently considered being well established [16]. This underlines the need for fluorescence quantum yield standards with certified Φ_f values for the ultraviolet (UV), visible (vis), and near-infrared (NIR) spectral region, which are not available yet.

$$\Phi_f = \frac{N_{em}}{N_{abs}} \quad (1)$$

The use of a Φ_f standard that presents the least predictable source of uncertainty for relative optical measurements can be circumvented by measuring N_{em} and N_{abs} absolutely with an integrating sphere setup [11,15,17–27]. This method is expected to gain in popularity due to the recent availability of commercialized integrating sphere setups [11,17,22]. The reliability of such measurements that imposes, e.g., more stringent requirements on the range of linearity of the detection system as conventional fluorescence measurements, depends to a considerable extent on the accuracy of the instrument correction curves implemented by the instrument manufacturer. Moreover, concentration-dependent dye- and matrix-specific reabsorption effects must be considered for fluorophores with a small Stokes shift as found for the majority of bioanalytically relevant labels and probes [10,27].

Alternatively, Φ_f can be obtained indirectly by measuring the fraction of the incident radiant power converted into heat using photothermal methods like thermal lensing [28–33] not further detailed here and photoacoustic spectroscopy (PAS) [22,34–37]. PAS exploits the generation of sound after illuminating a material with non-stationary (modulated or pulsed) radiation. Basically, the periodic pressure wave caused by the temperature rise in the sample due to the absorbed energy that is not emitted, is measured with a microphone or another acoustic transducer attached to the sample cell. Although PAS, as well as thermal lensing, are often termed absolute methods, the heat conversion efficiency of a fluorophore is measured relative to that of a non-emissive or completely quenched reference dye (conversion efficiency of 100%) in the same matrix and absorbing at the same wavelength to realize similar thermal transport coefficients. Main challenges of pulsed laser PAS are fluctuations in the incident radiant power, which limit the precision of the measurements, and the need for laser excitation that can induce photodecomposition [15,36]. Other practical problems for routine applications include a good and reproducible contact between sample and acoustic transducer, a close match between the thermal transport coefficients of sample and reference, and difficulties to detect small temperature changes. Moreover, the linearity of the photoacoustic signal must be ensured and additional absorption and emission measurements including spectral corrections are required.

The increasing demand for quantum yield standards covering the UV/vis/NIR spectral region requires the determination of Φ_f values of photophysically well characterized dyes under exactly specified measurement conditions with different, preferably absolute methods and known measurement uncertainties. Although the Φ_f values of fluorophores such as fluorescein, rhodamine 6G, rhodamine B, diphenylanthracene, and cresyl violet were measured with optical and photothermal techniques, typically, miscellaneous experimental conditions were used like different dye concentrations due to the varying sensitivities of these methods [15,16]. However, this parameter is directly linked to the size of reabsorption effects and the extent of aggregate formation which can both affect the reliability of Φ_f values. Also, fluorophore purity was often not specified. Really comparative measurements using the same dye (from the same batch) at identical concentration(s) have been scarcely performed [22,36]. As a first step to establish quantum yield standards for the UV/vis/NIR, we determine the Φ_f values of rhodamine 6G (R6G), which is one of the best characterized fluorophores with an excitation wavelength-independent quantum yield, with a new integrating sphere setup enabling direct and indirect illumination of the sample and pulsed laser PAS using identical measurement conditions. This systematic comparison was performed for different concentrations of R6G in ethanol and water to derive the influence of reabsorption effects and dye aggregation on the resulting Φ_f values. In addition, measurements of relative and absolute fluorescence quantum yields were conducted with a calibrated spectrofluorometer and a commercialized integrating sphere setup.

2. Experimental

2.1. Materials

Rhodamine 6G (R6G; batch number 119202) and Rh101 (batch number 019502) were purchased from Lambda Physik GmbH and Basic Fuchsin (batch number MKAA2788C9) from Sigma–Aldrich GmbH. All dyes were used without further purification. Ethanol was of spectroscopic grade and obtained from Sigma–Aldrich. For the preparation of the aqueous dye solutions, we used bidistilled water (pH ca. 7.0). Prior to use, all solvents were checked for luminescent impurities. Potassium iodide (KI) used for the quenching of the R6G fluorescence for PAS was purchased from Sigma–Aldrich GmbH. All optical spectroscopic measurements were performed at $T = 298 \pm 1$ K with 10 mm × 10 mm quartz cuvettes (Hellma GmbH) using air-saturated solutions. For the aggregation studies, the absorption measurements were performed in cuvettes of pathlengths of 10 mm and 1 mm. For PAS measurements, 4 mm × 10 mm quartz cells of were used.

2.2. Methods

2.2.1. Dye purity

HPLC measurements of R6G and R101 were performed with a HPLC system from Knauer (WellChrom solvent organizer K-1500, WellChrom HPLC pump K-1001; $T = 296$ K, $p = 200$ bar) equipped with a diode array detector (DAD; K-2800, WellChrom) and a EC 250/4 column from Machery-Nagel packed with NUCLEODUR C-18 gravity (particle diameter 5 μm) [11]. The purity of R6G was determined to >98.5% (480 nm and 530 nm) and the purity of R101 to 95.5% (525 nm) and 97.4% (565 nm). The purity of Basic Fuchsin was >88% as certified by the Biological Stain Commission.

2.2.2. Absorption and relative fluorescence measurements

Absorption spectra of the dye solutions used for the fluorescence studies were recorded on a calibrated Cary 5000 spectrometer (Varian Inc.). The absorption spectra of the samples employed for the PAS measurements that also provided the basis for the control of the photostability of the compounds, were obtained with a DU650 spectrophotometer (Beckman Inc). Spectrally corrected fluorescence spectra were measured with a previously described custom-modified Spectronics Instruments' 8100 spectrofluorometer equipped with Glan Thompson polarizers in the excitation and emission channel set to 0° and 54.7°, respectively [10,38].

2.2.3. Relative fluorescence quantum yields

The relative fluorescence quantum yield was calculated as previously described [10], following Eq. (2)

$$\Phi_{f,x} = \Phi_{f,st} \frac{F_x}{F_{st}} \frac{f_{st}(\lambda_{ex,st})}{f_x(\lambda_{ex,x})} \frac{n^2_{water}}{n^2_{EtOH}} \quad (2)$$

The subscripts 'st' and 'x' denote standard (R6G in EtOH; use of absolutely determined Φ_f value, see next section, as $\Phi_{f,st}$) and sample (R6G in water), $f(\lambda_{ex})$ is the absorption factor at the excitation wavelength, and n is the refractive index of the solvent(s). F

represents the integral spectral fluorescence photon flux $q^{f}_{p,\lambda}(\lambda_{em})$ at the detector that is calculated from the blank and dark-count corrected signal of the emission detector $I_u(\lambda_{em})$ multiplied with the photon energy hc_0/λ_{em} and divided by the instrument's spectral responsivity $s(\lambda_{em})$.

2.2.4. Integrating sphere setup for absolute measurements of Φ_f

The absolute Φ_f of R6G in ethanol and bidestilled water (excitation at 500 nm) and of R101 in ethanol (excitation at 525 nm), see Eq. (1), were measured as a function of dye concentration using a custom-designed calibrated integrating sphere setup at BAM. This setup consists of a xenon lamp coupled to a single monochromator and a six inch Spectraflect-coated integrating sphere (Labsphere GmbH) coupled with a quartz fiber to an imaging spectrograph (Shamrock 303i, Andor Inc.) and a Peltier cooled thinned back side illuminated deep depletion charge coupled device (CCD array). A reference detector was implemented to account for fluctuations of the radiant power reaching the sample. The sample or blank (i.e., the pure solvent) in a conventional 1 cm quartz cuvette cell was mounted into the center of the integrating sphere. The integrating sphere setup enables direct [11,22] and indirect [19] sample illumination as well as a combination of both illumination conditions [17,25]. For direct excitation, the excitation light was focused into the middle of the sample, see Fig. 1. For indirect sample illumination, the excitation light was focused near the middle (sample position) of the integrating sphere with the aid of an additional off-axis parabolic mirror and an additional sphere port, thereby carefully avoiding direct illumination. For the determination of Φ_f, see Eq. (3), the incident spectral radiant power of the direct and indirect illumination were adjusted to equal each other. Subsequently, both the incident and the transmitted spectral radiant power at 500 nm and the emission spectrum of the sample and the blank (solvent-filled cuvette) were measured at identical instrument settings (e.g., excitation wavelength, temperature, monochromator bandwidth) within a single scan for sample and blank under both illumination conditions.

The emitted integral photon flux $F^{dir,indir}$ was calculated from Eq. (3) for direct (superscript *dir*) and indirect illumination (superscript *indir*), see also Fig. 1 (right panel). The reliability of $s(\lambda_{em})$ of the integrating sphere-detection system was ensured by comparing the corrected emission spectra of dilute solutions of R6G obtained with the integrating sphere setup and a calibrated spectrofluorometer.

$$F = \int_{\lambda_{em_1}}^{\lambda_{em_2}} q^{f}_{p,\lambda}(\lambda_{em})\, d\lambda_{em} = (hc_0)^{-1} \int_{\lambda_{em_1}}^{\lambda_{em_2}} \frac{I_u(\lambda_{em})}{s(\lambda_{em})} \lambda_{em}\, d\lambda_{em} \quad (3)$$

The integral absorbed photon flux F_{abs} for direct and indirect illumination (gray area in the right panel of Fig. 2) was obtained from the difference of the spectrally corrected signals of the blank (I_{CB}) and the sample (I_{CS}) in the wavelength range of the excitation light (Fig. 1, right), see Eq. (4).

$$F^{dir,indir}_{abs} = F_0 f(\lambda_{ex}) f^{indir}(\lambda_{ex}) = \int_{\lambda_{ex_1}}^{\lambda_{ex_2}} q_{abs}(\lambda_{ex})\, d\lambda_{ex}$$

$$= \int_{\lambda_{ex_1}}^{\lambda_{ex_2}} \frac{\lambda_{ex}}{hc} (I_{CB}(\lambda_{ex}) - I_{CS}(\lambda_{ex}))\, d\lambda_{ex} \quad (4)$$

For direct illumination, the absorbed photon flux is proportional to the absorption factor $f(\lambda_{ex})$ and to the absorption factor for indirect illumination $f^{indir}(\lambda_{ex})$ for which the optical pathlength is not defined. F_0 presents the integral spectral photon flux measured with a blank (solvent-filled cuvette) and is identical for direct and indirect illumination. Absolute Φ_f measurements using direct and indirect excitation are combined in Eq. (5). Derivation of Eq. (5) equals the formula of de Mello et al. [25] despite the slightly different measurement principles used.

$$\Phi_f = \frac{F^{dir} - (1 - f(\lambda_{ex}))F^{indir}}{f(\lambda_{ex})F_0} \quad (5)$$

2.2.5. Fluorescence lifetime measurements

Fluorescence lifetimes were measured with a custom-built laser pulse fluorometer with picosecond time resolution with a typical experimental accuracy of ±3 ps for an excitation wavelength at 532 nm [39,40]. The resulting fluorescence was collected in a 0°/90° geometry with the polarizer set to 54.7° (magic angle condition). The quality of the fits was judged from the value of χ^2 and by the randomness of the weighted residuals. The χ^2 values observed for monoexponential fits of our fluorescence decay curves were 1.01.

2.2.6. Photoacoustic (PA) setup

The PA setup shown in Fig. 2 (left panel) consists of a pulsed frequency-doubled, Q-switched Nd:YAG laser (SL280 Spectron Laser System, Frankfurt, Germany, 532 nm, 6 ns, 10 Hz) focused with a plano-convex lens (100 mm focal length) into a 10 mm glass cuvette (filled with 800 μl of a dye or standard solution) that is coupled to a homemade piezoelectric PVDF (polyvinylidene fluoride) transducer on one side (side-on detection) [41], linked via an amplifier (HCA-100M-50k-C high speed current amplifier, Femto, Berlin, Germany) to a digital oscilloscope that records the PA signal. A fraction of the laser beam was directed onto a pyroelectric detector (Pyroelectric J25LPMB, Laser System, Dieburg, Germany) for the on line-determination of the laser pulse energy. The oscilloscope was triggered by the Q-switch trigger signal of the Nd:YAG laser.

Pulsed laser PAS relies on the absorption of a short laser pulse and subsequent measurement of the non-radiative thermal relaxation by the detection of ultrasonic pressure pulses. The amplitude of a pressure pulse p

$$p(\lambda_{ex}) = \zeta \cdot \frac{\beta \cdot v_s^2}{C_p \cdot l} \cdot F_0 \cdot f(\lambda_{ex}) = \zeta \cdot \alpha(\lambda) \quad (6)$$

depends on the ratio ζ of the radiative and non-radiative (thermal) relaxation constants k_f and $k_{th,}$ i.e., $\zeta = (k_{th}/(k_{th} + k_f))$, the laser fluence F_0, the pathlength l of the sample, and the matrix-specific quantities thermal expansion coefficient β, speed of sound v_s, and heat capacity C_p as well as on the absorption factor $f(\lambda_{ex})$. For a fluorescent sample consisting of a single absorbing and emitting species, Eq. (6) transforms into Eq. (7).

$$p(\lambda) = \alpha(\lambda) \cdot q \cdot \left(1 - \frac{\bar{\nu}_{em}}{\nu_{ex}} \Phi_f\right) \quad (7)$$

In Eq. (7), q is a sample- and instrument-related constant, ν_{ex} is the wavenumber of the excitation, $\bar{\nu}_{em}$ is the average emission wavenumber of the spectrally corrected emission spectrum of the fluorophore, and Φ_f its fluorescence quantum yield. α is directly proportional to the fraction of light absorbed in the part of the sample that yields the PA signal and the term in brackets represents the photoactivity loss of the PA signal. The heat conversion efficiency of a fluorophore is measured relative to that of a non-emissive or completely quenched dye (conversion efficiency of 100%) in the same matrix and absorbing at the same wavelength to cancel out the matrix-specific quantities β, v_s, and C_p as well as q in Eq. (7) yielding Eq. (8) [15,37].

$$\Phi_f = \frac{\nu_{ex}}{\bar{\nu}_{em}} \cdot \left(1 - \frac{p_{sample}(\lambda_{ex})}{p_{reference}(\lambda_{ex})}\right) \quad (8)$$

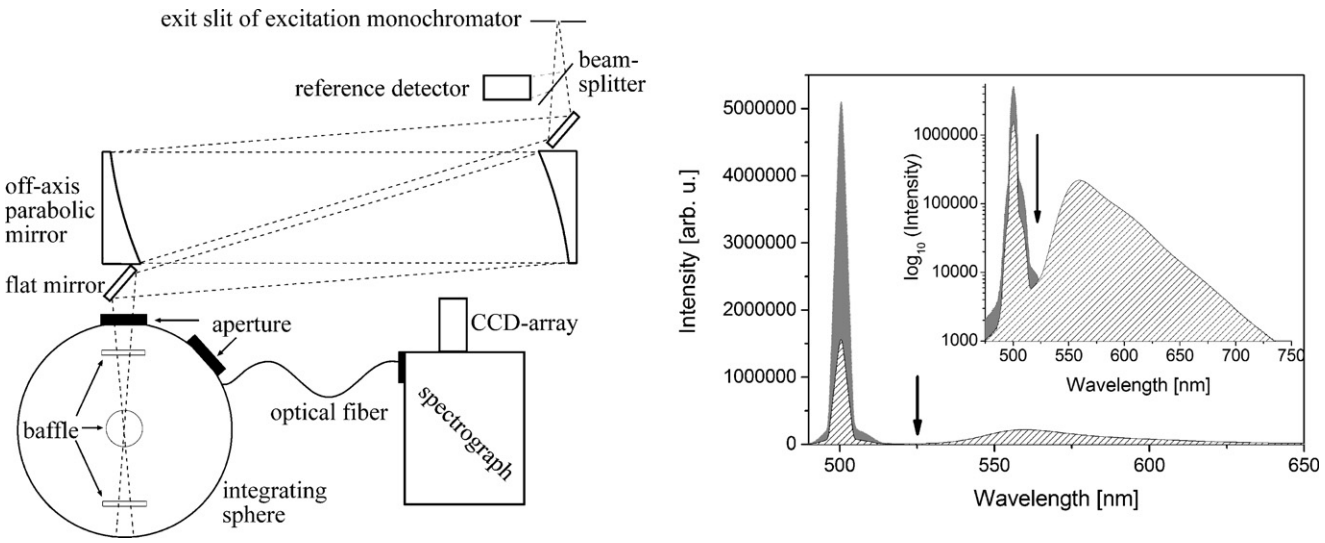

Fig. 1. (Left) Scheme of the integrating sphere setup for direct sample illumination. (Right) Separation of the spectral regions of excitation and emission indicated by the arrow.

3. Results and discussion

For the establishment of the methodical basis for fluorescence quantum yield standards for the UV/vis/NIR, we determined the fluorescence quantum yields of R6G in ethanol and water as a function of dye concentration with relative and absolute optical measurements and PAS in order to derive limitations and sources of uncertainty of each method and to evaluate the comparability of the resulting data.

3.1. Photoacoustic spectroscopy (PAS)

Essential for the reliable determination of the fluorescence quantum yields with pulsed laser PAS is the sensitivity of the setup, its long-term stability, and the reproducibility of the measurement conditions for sample and reference dye. Other potential sources of uncertainty are detailed in the next section. Key parameters to achieve this are a suitable and reproducible sensor arrangement, choice of an eligible reference dye to realize closely resembling measurement conditions for sample and reference, and use of a sufficiently low incident radiant power of the laser in conjunction with photochemically stable chromophores to minimize dye photodecomposition [15].

3.1.1. Sensor-cell arrangement

Various sensor-cell arrangements were tested with respect to the quality of the contact between sample and acoustic transducer and its reproducibility. This included (i) a free standing piezoelectric PVDF sensor head where coupling between sample and sensor was realized with an ultrasonic gel, providing the possibility to remove the measurement cell easily, (ii) use of a PMMA (poly[methyl methacrylate]) cuvette coupled with a PVDF sensor, and (iii) use of quartz cells for small sample volumes as detailed in Supporting information (SI). The latter setup gave the best results in our case. The PA signal of an aqueous solution of 1×10^{-6} M Basic Fuchsin, a non-emissive dye, detected perpendicular to the laser beam that is shown in Fig. 2 (right panel) underlines the sensitivity of the modified setup. The peak at ~2 μs, the amplitude of which varies with the absorbance and laser pulse energy results from the PA effect.

3.1.2. Choice of optimum reference dye: non-emissive absorber vs. quenched fluorophore

Prerequisites for a suitable non-emissive reference dye include closely matching absorption properties of reference dye and fluorophore in the same solvent, here ethanol and water, and a sufficient photochemical stability of both dyes in these solvents. Accordingly, we assessed the spectroscopic properties of Basic

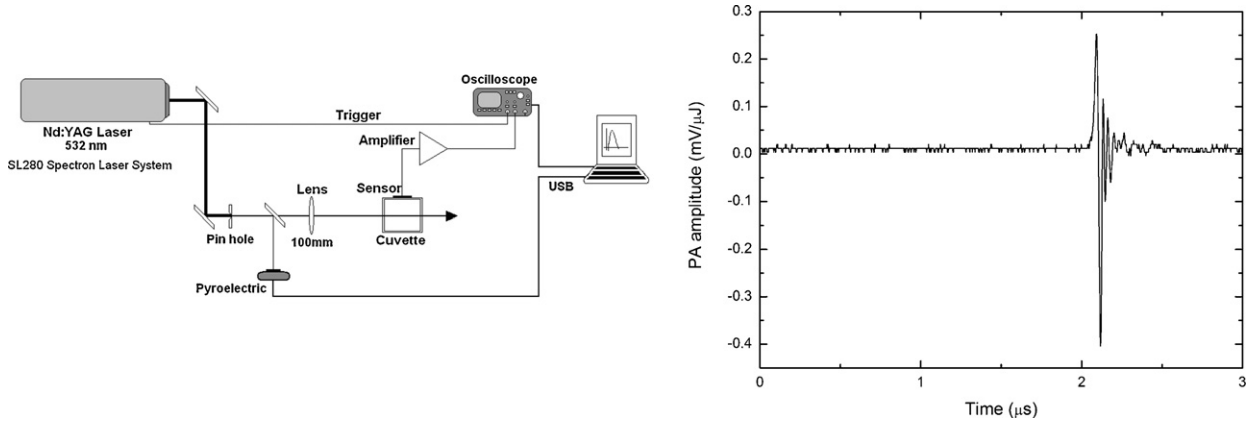

Fig. 2. (Left) Scheme of the PAS setup. (Right) Characteristic PA signal of an aqueous solution of Basic Fuchsin excited at 532 nm, the dye concentration was 1×10^{-6} M.

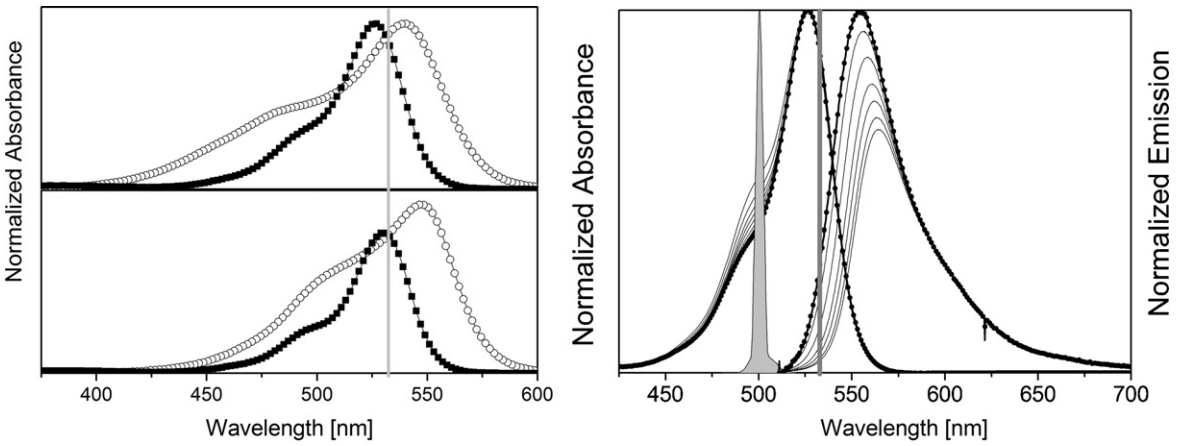

Fig. 3. (Left) Absorption spectra of R6G (full squares) and Basic Fuchsin (open circles) in water (top) and in EtOH (bottom) normalized at 532 nm used as excitation wavelength for PAS (vertical solid gray line). (Right) Absorption spectra (normalized at band maximum) and emission spectra (normalized at 620 nm) of R6G in water measured with an integrating sphere setup with spectra of the lowest dye concentration being highlighted (solid circles); the excitation light peaks employed for the calculation of the number of absorbed photons for the integrating sphere measurements (light gray peak at 500 nm) and the excitation wavelength of 532 nm used for PAS (dark gray line) are indicated. The concentrations of the dye solutions follow from Table 1.

Fuchsin in both solvents and performed fluorescence quenching studies with R6G. The normalized absorption spectra of R6G and Basic Fuchsin in EtOH and in water are displayed in Fig. 3 (left panel). The relatively good match between the absorption bands of both dyes in these solvents underlines the principal suitability of Basic Fuchsin as reference dye. Emission measurements performed with Basic Fuchsin at maximum slit widths of our fluorometer confirmed its non-emissive nature. Spectroscopic studies of R6G solutions revealed very similar absorption and emission spectra of R6G in water and in EtOH. Addition of even very high amounts of KI (concentrations up to 0.95 mol/l) to R6G in water required for the quenching studies did not result in spectral changes in absorption. Collisional quenching of the emission of R6G by KI is not possible in ethanol due to the considerably diminished solubility of KI in this solvent (0.27 mol/l) as compared to water (8.6 mol/l).

Addition of KI to R6G in water results in a concentration-dependent reduction in fluorescence intensity and lifetime, see SI (Fig. 4S), yielding a quenching constant of k_q of ca. 1.3×10^{10} [1/s]. The fluorescence lifetime of R6G in bidestilled water amounts to 3.79 ns, closely matching the reported lifetime of this dye of 4.08 ns in water [33]. Although addition of KI results in a strong diminution in emission, the emission of R6G remained detectable even at high concentrations of KI (0.95 mol/l). In addition, at concentrations of KI $\geq$ 0.75 mol/l, the solubility of R6G in water was increasingly affected by the presence of KI, with the dye starting to adsorbed onto the cuvette walls. This undesired influence of KI can be also observed in the Stern–Volmer plot shown in the SI (Fig. 4S;right panel, deviation of the data points from straight line at high KI concentrations, i.e., downward bending). Hence, PAS experiments were solely performed with Basic Fuchsin as reference dye.

3.1.3. Photostability

Dye photostability always presents a critical issue for measurements with laser excitation. In order to ensure dye photostability, absorption spectra of the sample and reference dye for the PAS studies were measured before and after each measurement for different laser pulse energies. To minimize photodegradation of the dyes studied, the laser energy was always kept below 250 μJ. A laser fluence of below 0.5 J/cm^2 assured a photodecomposition below 5% with respect to the starting dye concentration. Also a linear relationship between the PA signal amplitude and the laser energy was assured (see SI, Fig. 3S), indicating the absence of saturation effects [42].

3.2. Determination of Φ_f with optical methods and PAS

Major factors governing the accuracy of the determination of Φ_f with optical methods and PAS include instrument characterization and calibration, the stability of the excitation light intensity, and previously discussed method-inherent sources of variation such as the quality of the contact between sample and detector in the case of PAS or the need for direct or indirect illumination of the sample for absolute optical measurements with an integrating sphere setup [25]. Moreover, dye- and matrix-specific and concentration-dependent reabsorption and aggregation can play an important role. For this comparison, contributions from dye impurities are expected to influence both methods too a comparable extent due to the use of identical dye batches for our studies.

3.2.1. Absolute optical determination of Φ_f – direct and indirect sample illumination

As the number of absorbed and emitted photons are measured within a single scan (see Section 2 and Fig. 1), proper separation of the transmitted excitation light and the emission spectrum is essential. This determines also the choice of a suitable excitation wavelength (see SI, Fig. 1S). Hence, R6G was excited at 500 nm and not at 532 nm as employed for PAS. As for the measurement of absolute fluorescence quantum yields, often direct and indirect sample illumination (see Fig. 1 and Eqs. (4) and (5)) is recommended, especially for solid and scattering materials [25], in a first step, we investigated the influence of both types of excitation on the Φ_f values resulting for transparent and relatively dilute dye solutions of R6G in water (concentration range of 9.3×10^{-7} M to 2.3×10^{-5} M). As summarized in Table 1, the Φ_f data obtained for both illumination geometries are in excellent agreement except for the lowest dye concentration of 9.3×10^{-7} M. For this concentration, in the case of indirect illumination, only 2.7% of the excitation light is absorbed, whereas in the case of direct illumination, the fraction of absorbed light amounts to 7.7%. Obviously, for dilute dye solutions, the illumination conditions used for the integrating sphere measurements play only a very minor role. The diminution in Φ_f with increasing dye concentration observed for all types of illumination is caused by reabsorption effects and dye aggregation as discussed in the following sections.

Table 1
Comparison of the absolute fluorescence quantum yields of R6G in water determined with the integrating sphere setup using direct and indirect sample illumination.

c [mol/l]	Direct illumination (Eq. (1))	Indirect illumination (Eq. (1))	Direct and indirect illumination (Eq. (5))
9.27E−07	0.84	0.91	0.81
2.69E−06	0.77	0.77	0.77
6.04E−06	0.75	0.77	0.75
1.08E−05	0.69	0.70	0.69
1.44E−05	0.66	0.65	0.66
1.85E−05	0.62	0.61	0.62
2.32E−05	0.59	0.58	0.59

3.2.2. Reabsorption effects

Reabsorption effects can influence both PAS and absolute optical measurements of Φ_f. Multiple reflections of emitted photons inside an integrating sphere increase the distance of emitted photons traveled prior to detection, and thus the reabsorption probability (see emission spectra in Fig. 3, right panel). Hence, for the majority of fluorescent materials, measured absolute Φ_f values need to be corrected for reabsorption (see SI, Eq. (1S)). For PAS, reabsorption of emitted fluorescence radiation can lead to an increased PA signal. To minimize such effects, PA cells with a limited cross section of 2 mm, corresponding to the optical path length of the emitted light, were used.

3.2.3. Dye aggregation

R6G can form dimers and higher aggregates in water within the concentration range (see Table 1) used by us for the quantum yield measurements. This is indicated in Fig. 3 (right panel) by a concentration-dependent change in the spectral shape of the absorption band of R6G and the characteristic appearance of a new absorption band at the vibronic shoulder of the dye's main absorption peak (see also SI, Fig. 1S). The contribution of the absorption of these non- or barely emissive dimers ($\Phi_{f,D} = 6 \times 10^{-4}$) [43] to the overall absorption of the dye solution at the excitation wavelength of 500 nm can considerably affect the reliability of the resulting Φ_f values [15,37,44]. Proper consideration of the aggregate absorption requires knowledge of the concentration of the dye species formed in solution and thus, the aggregation constant K_d [45–49]. For the determination of K_d, we measured the absorption spectra of R6G in water in the concentration range of 3.3×10^{-4} M to 6.4×10^{-7} M (see SI, Fig. 1S). The isosbestic point obtained indicates the presence of only two spectroscopically distinguishable species, the R6G monomer and dimer. From these data, K_d was determined to 3.0×10^3 M^{-1} in excellent agreement with other literature data [45,50–52]. Subsequently, the concentration of the R6G monomers and dimers, their absorption spectra (see SI, Fig. 2S), and their contribution to the absorption at the excitation wavelength were calculated as detailed in the SI and used for the correction of the measured absolute fluorescence quantum yields for dimer absorption.

In ethanol, the aggregation tendency of R6G is significantly lower as compared to water. Reported values for the dimerization constant of R6G in this solvents lie in the range of 0.11–6.2 M^{-1} [53]. Accordingly, in the concentration range used by us for the integrating sphere and PAS measurements, i.e., 5.6×10^{-7} M to 2.3×10^{-5} M, no R6G aggregates should be formed. The absence of aggregates was additionally confirmed by dilution studies comparing the normalized absorption spectra of differently concentrated dye solutions.

3.2.4. Optically measured absolute fluorescence quantum yields

Fig. 4 summarizes the fluorescence quantum yields of R6G in water (left panel) and ethanol (right panel) as measured (Φ_f value of solution or apparent Φ_f), the Φ_f values corrected for dimer absorption at the excitation wavelength (water only), and the reabsorption-corrected Φ_f data (dimer absorption- and reabsorption corrected Φ_f values of R6G in water and reabsorption corrected-Φ_f values of R6G in ethanol). The undisturbed emission spectra of R6G dissolved in water and ethanol used to correct reabsorption effects are shown in Fig. 5S in the SI. For the chosen dye concentrations, fluorescence diminishing fluorescence energy transfer from emissive monomers to non-emissive or barely emissive dimers that are significant, e.g., in dye-biomolecule conjugates [48,49,54] can be neglected in solution. For the highest dye concentrations used, the smallest mean distance of donor and acceptor is in the range of 42 nm whereas the Förster radius of R6G was reported to be in the order of 4.1 nm (critical transfer concentration $c_0 = 5.6 \times 10^3$ M) [43] to 6.8 nm [55].

Our corrections yield a mean value of the fluorescence quantum yield of monomeric R6G of 0.83 in water and 0.92 in ethanol (Fig. 4, full circles). The strong deviations between the measured apparent Φ_f and the corrected Φ_f that amount to ca. 35% for R6G in water for the highest dye concentration used, underline the need for corrections to accomplish really reliable absolute optical measurements.

3.2.5. PAS measurements of fluorescence quantum yields

The concentration dependence of the PA amplitudes of Basic Fuchsin and R6G in water and ethanol are summarized in Fig. 6S in the SI. For both dyes, the PA amplitudes reveal a linear concentration dependence in the concentration range of 10^{-7} to 10^{-5} M. In aqueous solution, the contributions of R6G dimers to the measured absorbance at 532 nm is almost negligible for dye concentrations in the 10^{-6} M range (<1%) and rise to <3.5% for concentrations $<2 \times 10^{-5}$ M. As to be expected from the absorption spectra of the monomers and dimers (see Fig. 5 and Fig. 1S in the SI) and an excitation wavelength of 532 nm, aggregation does not seemingly affect the measured PA signals and thus, the resulting Φ_f values. Using Eq. (7) with slopes calculated by a linear fit in the used concentration range, the fluorescence quantum yield of R6G was determined to 1 in ethanol and to 0.91 in water.

3.2.6. Measurement uncertainties

Assessment of the comparability of the fluorescence quantum yields obtained with PAS and optical spectroscopy requires knowledge of the respective measurement uncertainties, calculated with Eq. (7S) (see SI). All values were rounded to the second digit. For the absolute optical measurements with our integrating sphere setup, the systematic uncertainties are estimated to 5%. These uncertainties include contributions from the calibration of the setup, the linearity of the detection system, and the homogeneity of the reflectivity of the sphere walls. In conjunction with the repeatability of Φ_f measurements ca. 1.5%, including sample positioning, and fluctuations of the incident radiant power, this yields absolute fluorescence quantum yields of 0.92 ± 0.05 for R6G in EtOH and 0.83 ± 0.04 in water.

The systematic uncertainties of PAS were assumed to be 5%, considering mainly the photostability of the sample and reference dye

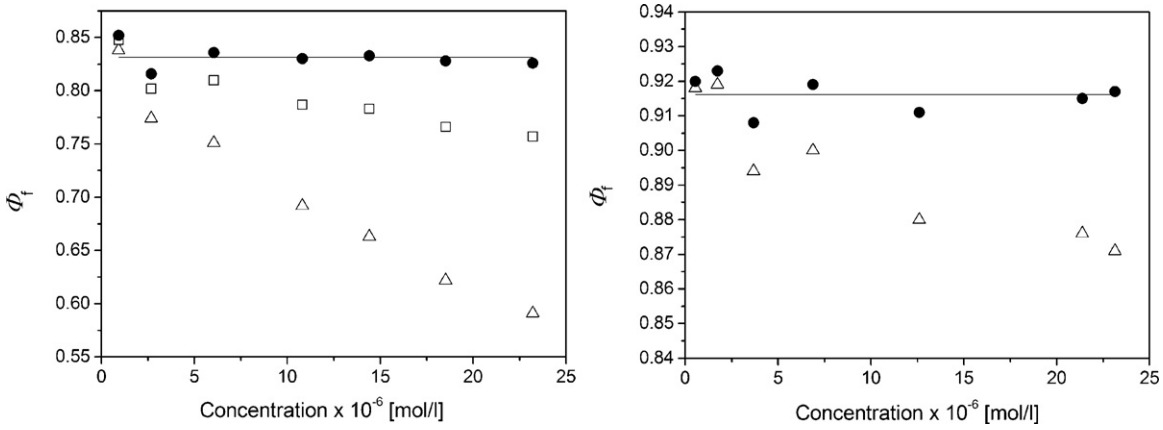

Fig. 4. Optically measured (open triangles), dimer absorption- (open squares) and reabsorption- (full circles) corrected, concentration-dependent absolute fluorescence quantum yields of R6G in water (left) and in ethanol (right). The solid lines indicate the mean Φ_f value.

and the linearity of the PA signal. Together with the repeatability of ca. 4% for PAS measurements in EtOH and ca. 7% for water, including fluctuations of the incident radiant power of the pulsed laser light, and uncertainties arisng from the cell positioning and absorption measurements which required the transfer of the dye solution into the measurement cell, this results in fluorescence quantum yields of 1 ± 0.06 for R6G in ethanol and 0.91 ± 0.08 for R6G in water.

3.2.7. *Quantum yield comparison*

The fluorescence quantum yields obtained by us are in good agreement with the Φ_f values of 0.82–0.97 reported for water [33,43,50,56–58] and 0.87–1 for ethanol [17,19,33,56,57,59]. For both systems studied, the fluorescence quantum yields of R6G measured with PAS exceed the values obtained optically. Nevertheless, despite these deviations in the absolute numbers of about 10%, the results of the PAS and absolute optical measurements agree within the uncertainties derived for each method. In addition, the fluorescence quantum yield of R6G in EtOH was determined by us only recently with a commercialized integrating sphere setup to $\Phi_f = 0.90 \pm 0.05$ and with two relative optical methods to $\Phi_f = 0.89 \pm 0.05$ and 0.89 ± 0.06 [10]. These data agree very well with the value found with our new integrating sphere setup. In order to additionally verify our absolute Φ_f values, we measured the absolute fluorescence quantum yield of the recommended quantum yield standard R101 in ethanol that is being used by us for several years as gold standard for our relative quantum yield measurements [4]. The resulting Φ_f value of 0.92 coincide excellently with previous measurements using a commercialized integrating sphere setup from Hamamatsu ($\Phi_f = 0.90 \pm 0.07$; excitation at 525 nm) [11] and with recent measurements of the group of Tobita [22]. Also, relative optical measurements with a calibrated spectrofluorometer using the same batch of R101 and quinine sulfate dihydrate as quantum yield standard led to Φ_f of 0.91 [60].

Moreover, the relative determination of the fluorescence quantum yield of R6G in water using R6G in ethanol as standard (using $\Phi_f = 0.92$ as determined optically and $\Phi_f = 1$ as obtained by PAS) yields relative fluorescence quantum yields of 0.83 and 0.91 that are also in excellent agreement with the data measured here. Hence, our measurements could provide a first hint that PAS may yield systematically higher fluorescence quantum yields as absolute optical measurements with an integrating sphere setup. To confirm this trend, further systematic measurements with fluorophores of known purity, varying fluorescence quantum yield and varying Stokes shift are required.

4. Conclusion and outlook

The fluorescence quantum yield of R6G in ethanol and water were determined to 1 ± 0.06 and to 0.92 ± 0.05 (EtOH; no dimers) and to 0.91 ± 0.08 and 0.83 ± 0.04 (water; formation of dimers) by photoacoustic and absolute optical spectroscopy. These data are in good agreement with the Φ_f values of 0.82–0.97 reported by other authors for R6G dissolved water [33,43,50,56–58] and 0.87–1 in the case of ethanol [17,19,33,56,57,59] and agree within the range of uncertainty. Prerequisites for the accomplished small measurement uncertainties include optimized setups and calibration procedures as detailed in the previous section with main factors being the tight and reproducible contact of the measurement cell and detector in the case of PAS and the consideration of reabsorption and aggregation effects. Nevertheless, these measurements yield a deviation of about 10% for both methods. This can point to a systematic variation of optical and photoacoustic measurements that needs to be assessed by systematic comparative measurements of fluorophores differing in the size of their fluorescence quantum yields and their Stokes shift. Alternatively, both methods could be combined with a single setup, thereby also paving the road for the improved characterization of innovative multi-modal contrast agents for PA and fluorescence imaging or tomography. These measurements also emphasize the need to confirm the accuracy of the quantum yield values of many commonly used standards and simple protocols for the performance of quantum yield measurement with different techniques.

Advantageous of PAS that is well suited for the measurement of fluorescence quantum yields of dilute dye solutions, is the relatively simple calibration of the PAS setup with a non-fluorescent reference and the minimum signal distortions by reabsorption effects due to the measurement geometry and high sensitivity of our setup. Limitations present the tight coupling between PA sensor and measurement cell, hampering routine handling and easily affecting the repeatabilities of measurements, and the need for additional measurements of the absorption and emission spectrum of the sample (three independent measurements are necessary to determine the quantum yield by PAS), rendering measurements time-consuming and potentially leading to enhanced measurement uncertainties. Moreover, the high radiant power of the pulsed excitation light requires careful adjustment to minimize photodegradation. This can be critical for samples of reduced photochemical or thermal stability as typical for many bioanalytically relevant NIR dyes and fluorescent biomolecule conjugates.

Compared to PAS, absolute optical measurements with an integrating sphere setup are more efficient requiring less preparation effort. Generally, the integrating sphere method provides an improved flexibility, enabling the determination of the photoluminescence quantum yields of a broad variety of samples differing in size and shape and dye concentration. Also scattering, photostability, and heating of the sample are not critical. Other advantages include no need of a reference, no limits with respect to excitation wavelength due to the use of a xenon lamp (which could be principally overcome for PAS using tunable solid state lasers that are, however, comparatively expensive), and no need for extra absorption measurements. In addition, the emission spectrum is always recorded providing more spectroscopic information. As revealed by our results, for transparent dye solutions, absolute fluorescence quantum yields can be measured with direct sample illumination solely. Disadvantageous are the more tedious calibration of the setup with physical transfer standards (e.g., determination of the spectral responsivity of the sphere-detector ensemble, wavelength accuracy and range of linearity) and the need for the correction of reabsorption effects. Concerning accomplishable sensitivities, our integrating sphere setup seems to be less sensitive as the PAS setup using pulsed laser excitation due to the huge surface of our sphere (sphere diameter of 15 cm), yet with the use of a smaller sphere and/or a more intense excitation light source, this could be overcome.

Acknowledgements

We gratefully acknowledge financial support from the Federal Ministry of Economics and Technology (BMWI; MNPQ grants 22/06 and 17/07), the Deutscher Akademischer Austauschdienst (DAAD), and the Facultad de Ingeniería Universidad de Buenos Aires (FIUBA).

Appendix A. Supplementary data

Supplementary data associated with this article can be found, in the online version, at doi:10.1016/j.talanta.2011.12.051.

References

[1] J.R. Lakowicz, Principles of Fluorescence Spectroscopy, 3rd ed., Springer Science + Business Media, LLC, New York, 2006.
[2] B. Valeur, Molecular Fluorescence: Principles and Application, Wiley-VCH, Weinheim, 2002.
[3] U. Resch-Genger, M. Grabolle, S. Cavaliere-Jaricot, R. Nitschke, T. Nann, Nature Methods 5 (2008) 763–775.
[4] M. Grabolle, M. Spieles, V. Lesnyak, N. Gaponik, A. Eychmüller, U. Resch-Genger, Analytical Chemistry 81 (2009) 6285–6294.
[5] J.N. Demas, G.A. Crosby, Journal of Physical Chemistry 75 (1971) 991–1024.
[6] J.N. Demas, Measurement of Photon Yields, Academic Press, New York, 1982.
[7] C.A. Parker, W.T. Rees, Analyst 85 (1960) 587–600.
[8] R.A. Velapoldi, H.H. Tonnesen, Journal of Fluorescence 14 (2004) 465–472.
[9] A. Heckmann, S. Dummler, J. Pauli, M. Margraf, J. Kohler, D. Stich, C. Lambert, I. Fischer, U. Resch-Genger, Journal of Physical Chemistry C 113 (2009) 20958–20966.
[10] C. Würth, M. Grabolle, J. Pauli, M. Spieles, U. Resch-Genger, Analytical Chemistry 83 (2011) 3431–3439.
[11] C. Wurth, C. Lochmann, M. Spieles, J. Pauli, K. Hoffmann, T. Schuttrigkeit, T. Franzl, U. Resch-Genger, Applied Spectroscopy 64 (2010) 733–741.
[12] U. Resch-Genger, P. deRose, Pure and Applied Chemistry 82 (2010) 2315–2335.
[13] P.C. DeRose, U. Resch-Genger, Analytical Chemistry 82 (2010) 2129–2133.
[14] U. Resch-Genger, K. Hoffmann, W. Nietfeld, A. Engel, J. Neukammer, R. Nitschke, B. Ebert, R. Macdonald, Journal of Fluorescence 15 (2005) 337–362.
[15] K. Rurack, in: U. Resch-Genger (Ed.), Standardization and Quality Assurance in Fluorescence Measurements. I: Techniques, Springer, Berlin, Heidelberg, 2008.
[16] A.M. Brouwer, Pure and Applied Chemistry 83 (2011) 2213–2228.
[17] L. Porrès, A. Holland, L.-O. Pålsson, A.P. Monkman, C. Kemp, A. Beeby, Journal of Fluorescence 16 (2006) 267–273.
[18] M.D. Galanin, A.A. Kufénko, V.N. Smorchkov, Y.P. Timofee, Z.A. Chizhikov, Optika I Spektroskopiya (USSR) 53 (1982) 683–689.
[19] L.S. Rohwer, J.E. Martin, Journal of Luminescence 115 (2005) 77–90.
[20] A.K. Gaigalas, L.L. Wang, Journal of Research of the National Institute of Standards and Technology 113 (2008) 17–28.
[21] G. Bourhill, L.O. Palsson, I.D.W. Samuel, I.C. Sage, I.D.H. Oswald, J.P. Duignan, Chemical Physical Letters 336 (2001) 234–241.
[22] K. Suzuki, A. Kobayashi, S. Kaneko, K. Takehira, T. Yoshihara, H. Ishida, Y. Shiina, S. Oishi, S. Tobita, Phys Chem Chem Phys 11 (2009) 9850–9860.
[23] J.C. Boyer, F. van Veggel, Nanoscale 2 (2010) 1417–1419.
[24] N.C. Greenham, I.D.W. Samuel, G.R. Hayes, R.T. Phillips, Y.A.R.R. Kessener, S.C. Moratti, A.B. Holmes, R.H. Friend, Chemical Physical Letters 241 (1995) 89–96.
[25] J.C. de Mello, H.F. Wittmann, R.H. Friend, Advanced Materials 9 (1997) 230–232.
[26] O.E. Semonin, J.C. Johnson, J.M. Luther, A.G. Midgett, A.J. Nozik, M.C. Beard, Journal of Physical Chemistry Letters 1 (2010) 2445–2450.
[27] H. Mattoussi, H. Murata, C.D. Merritt, Y. Iizumi, J. Kido, Z.H. Kafafi, Journal of Applied Physics 86 (1999) 2642–2650.
[28] T. Suzuki, M. Nagano, S. Watanabe, T. Ichimura, Journal of Photochemistry and Photobiology A: Chemistry 136 (2000) 7–13.
[29] M. Fischer, J. Georges, Chemical Physics Letters 260 (1996) 115–118.
[30] C.V. Bindhu, S.S. Harilal, V.P.N. Nampoori, C.P.G. Vallabhan, Modern Physics Letters B 13 (1999) 563–576.
[31] M. Fikry, M. Omar, L. Ismail, Journal of Fluorescence 19 (2009) 741–746.
[32] A. Kurian, S.D. George, C.V. Bindhu, V.P.N. Nampoori, C.P.G. Vallabhan, Spectrochimica Acta Part A: Molecular and Biomolecular Spectroscopy 67 (2007) 678–682.
[33] D. Magde, R. Wong, P.G. Seybold, Photochemistry and Photobiology 75 (2002) 327–334.
[34] T. Schmid, U. Panne, R. Niessner, C. Haisch, Analytical Chemistry 81 (2009) 2403–2409.
[35] Y. Yang, J. Li, X. Liu, S. Zhang, K. Driesen, P. Nockemann, K. Binnemans, Chemphyschem 9 (2008) 600–606.
[36] E.P. Tomasini, E. San Roman, S.E. Braslavsky, Langmuir 25 (2009) 5861–5868.
[37] D. Cahen, H. Garty, R.S. Becker, Journal of Physical Chemistry 84 (1980) 3384–3389.
[38] U. Resch-Genger, D. Pfeifer, C. Monte, W. Pilz, A. Hoffmann, M. Spieles, K. Rurack, J. Hollandt, D. Taubert, B. Schonenberger, P. Nording, Journal of Fluorescence 15 (2005) 315–336.
[39] Z. Shen, H. Rohr, K. Rurack, H. Uno, M. Spieles, B. Schulz, G. Reck, N. Ono, Chemistry: A European Journal 10 (2004) 4853–4871.
[40] Y.H. Yu, A.B. Descalzo, Z. Shen, H. Rohr, Q. Liu, Y.W. Wang, M. Spieles, Y.Z. Li, K. Rurack, X.Z. You, Chemistry: An Asian Journal 1 (2006) 176–187.
[41] T. Schmid, C. Helmbrecht, C. Haisch, U. Panne, R. Niessner, Analytical and Bioanalytical Chemistry 375 (2003) 1130–1135.
[42] J. Georges, N. Arnaud, L. Parise, Applied Spectroscopy 50 (1996) 1505.
[43] A. Penzkofer, W. Leupacher, Journal of Luminescence 37 (1987) 61–72.
[44] J. Pauli, T. Vag, R. Haag, M. Spieles, M. Wenzel, W.A. Kaiser, U. Resch-Genger, I. Hilger, European Journal of Medicinal Chemistry 44 (2009) 3496–3503.
[45] D. Toptygin, B.Z. Packard, L. Brand, Chemical Physics Letters 277 (1997) 430–435.
[46] U. Schobel, H.J. Egelhaaf, A. Brecht, D. Oelkrug, G. Gauglitz, Bioconjugate Chemistry 10 (1999) 1107–1114.
[47] M. Kubista, R. Sjoback, B. Albinsson, Analytical Chemistry 65 (1993) 994–998.
[48] U. Schobel, H.-J. Egelhaaf, A. Brecht, D. Oelkrug, G. Gauglitz, Bioconjugate Chemistry 10 (1999) 1107–1114.
[49] J. Pauli, M. Grabolle, R. Brehm, M. Spieles, F.M. Hamann, M. Wenzel, I. Hilger, U. Resch-Genger, Bioconjugate Chemistry 22 (2011) 1298–1308.
[50] M. Fischer, J. Georges, Spectrochimica Acta Part A: Molecular and Biomolecular Spectroscopy 53 (1997) 1419–1430.
[51] W. Inaoka, S. Harada, T. Yasunaga, Bulletin of the Chemical Society of Japan 53 (1980) 2120–2122.
[52] F.L. Arbeloa, P.R. Ojeda, I.L. Arbeloa, Journal of the Chemical Society-Faraday Transactions II 84 (1988) 1903–1912.
[53] P.R. Ojeda, I.A.K. Amashta, J.R. Ochoa, I.L. Arbeloa, Journal of the Chemical Society-Faraday Transactions II 84 (1988) 1–8.
[54] U. Schobel, H.-J. Engelhaaf, D. Fröhlich, A. Brecht, D. Oelkrug, G. Gauglitz, Journal of Fluorescence 10 (2000) 147–154.
[55] S.K. Hyun, S.J. Hong, S.E. Hyo, K.C. Gyu, K. Ung, S.K. Dong, Korean Physical Society 24 (1991) 302–305.
[56] W. Lahmann, H.J. Ludewig, Chemical Physics Letters 45 (1977) 177–179.
[57] A. Santhi, M. Umadevi, V. Ramakrishnan, P. Radhakrishnan, V.P.N. Nampoori, Spectrochimica Acta Part A: Molecular and Biomolecular Spectroscopy 60 (2004) 1077–1083.
[58] A. Chekalyuk, V. Fadeev, G. Georgiev, T. Kalkanjiev, Z. Nickolov, Spectroscopy Letters 15 (1982) 355–365.
[59] M.D. Galanin, A.A. Kutyonkov, V.N. Smorchkov, Y.P. Timofeev, Z.A. Chizhikova, Optika I Spektroskopiya 53 (1982) 683–690.
[60] K. Rurack, M. Spieles, Analytical Chemistry 83 (2011) 1232–1242.